

A method for computation of scattering amplitudes and Green functions of whole axis problems

Raúl Castillo-Pérez^a, Vladislav V. Kravchenko^b, Sergii M. Torba^b

^a Instituto Politécnico Nacional, Maestría en Telecomunicaciones, ESIME Zacatenco, CDMX, Mexico

^b Departamento de Matemáticas, Cinvestav, Unidad Querétaro, Querétaro, Mexico;

April 27, 2022

Abstract

A method for the computation of scattering data and of the Green function for the one-dimensional Schrödinger operator $H := -\frac{d^2}{dx^2} + q(x)$ with a decaying potential is presented. It is based on representations for the Jost solutions in the case of a compactly supported potential obtained in terms of Neumann series of Bessel functions (NSBF), an approach recently developed in [12]. The representations are used for calculating a complete orthonormal system of generalized eigenfunctions of the operator H which in turn allow one to compute the scattering amplitudes and the Green function of the operator $H - \lambda$ with $\lambda \in \mathbb{C}$.

1 Introduction

The Schrödinger one-dimensional operator $H := -\frac{d^2}{dx^2} + q(x)$ is considered with a potential q defined on the whole axis and decaying at infinity. A method for the computation of the eigenfunctions and generalized eigenfunctions as well as of scattering data and the Green function is developed. The need for the computation of the Green function and scattering data for this operator arises, e.g., in hydroacoustic problems (see, e.g., [2] and [3]) as well as when solving nonlinear evolution equation by means of the inverse scattering transform method (see [1]).

The simplest method for computing the Green function requires two linearly independent solutions (the Jost solutions) of the Schrödinger equation (see, e.g., [6]). However, the numerical realization of this method fails when the spectral parameter is relatively large. Another approach is based on the eigenfunction expansion of the Green function (see, e.g., [7, Sect. 5.3]) in which both the discrete and the continuous parts of the spectrum are represented. The computation of the generalized eigenfunctions (corresponding to the continuous spectrum) is in general a complicated task. In some cases the contribution of the discrete spectrum is considered asymptotically dominant and consequently the contribution of the continuous spectrum is neglected (see, e.g., [2] and [3]). In this way an intrinsic error is introduced in the computation.

Here we deal with the problem of computation of the scattering data and the Green function without neglecting the contribution of the continuous spectrum eigenfunctions, improving thus the accuracy of the computation. For this a recent result from [12] is used due to which the solutions of the Schrödinger equation

$$-y'' + q(x)y = \omega^2 y$$

are found in the form of Neumann series of Bessel functions (NSBF) admitting a uniform error estimate of approximation with respect to $\operatorname{Re} \omega$. This is especially convenient for computing the integrals arising in the eigenfunction expansion of the Green function.

The numerical implementation of the method is discussed, and some numerical illustrations are given.

The paper is organized as follows. In Section 2 we recall some known facts about the Schrödinger equation on the whole axis. In Section 3 we recall the main results from [12] and introduce a procedure for constructing solutions of the one-dimensional Schrödinger equation via the NSBF representation. In Section 4 the representation is used for calculating the Jost solutions for the Schrödinger equation with a compactly supported potential. In Section 5 we use the asymptotic expansions of the Jost solutions to improve the convergency of the integrals arising in the eigenfunction expansion of the Green function. In Section 6 the numerical implementation of the algorithm is discussed. Finally, some conclusions are provided.

2 Preliminaries

The one-dimensional Schrödinger operator

$$H := -\frac{d^2}{dx^2} + q(x)$$

is considered with q being a real-valued measurable function satisfying the condition

$$\int_{-\infty}^{\infty} (1 + |x|) |q(x)| dx < \infty. \quad (1)$$

Under this condition the Schrödinger equation

$$Hy(x) := -y''(x) + q(x)y(x) = \omega^2 y(x), \quad \omega \in R \quad (2)$$

possesses the solutions $y_1(x, \omega)$ and $y_2(x, \omega)$ with the following asymptotic behaviour at infinity

$$y_1(x, \omega) = e^{i\omega x} + o(1), \quad x \rightarrow \infty$$

and

$$y_2(x, \omega) = e^{-i\omega x} + o(1), \quad x \rightarrow -\infty$$

(see, e.g., [6]). The functions $y_1(x, \omega)$ and $y_2(x, \omega)$ are frequently referred to as the Jost solutions. They can be analytically extended onto $\text{Im } \omega \geq 0$ with this asymptotics [4].

For real $\omega \neq 0$ two fundamental sets of solutions can be constructed

$$\{y_1(x, \omega), \quad y_1(x, -\omega)\}$$

and

$$\{y_2(x, \omega), \quad y_2(x, -\omega)\}.$$

Note that

$$y_1(x, -\omega) = \overline{y_1(x, \omega)} \quad \text{and} \quad y_2(x, -\omega) = \overline{y_2(x, \omega)}.$$

These two fundamental sets are related by the equalities

$$y_2(x, \omega) = a(\omega)y_1(x, -\omega) + b(\omega)y_1(x, \omega),$$

$$y_2(x, -\omega) = \overline{b(\omega)}y_1(x, -\omega) + \overline{a(\omega)}y_1(x, \omega)$$

where $a(\omega)$ and $b(\omega)$ are called the transmission and the reflection coefficients respectively [4]. The coefficients satisfy the equality [6]

$$|a(\omega)|^2 = 1 + |b(\omega)|^2.$$

The transmission coefficient can be expressed in terms of the Wronskian of the solutions $y_1(x, \omega)$ and $y_2(x, \omega)$,

$$a(\omega) = -\frac{1}{2i\omega} (y_1'(x, \omega)y_2(x, \omega) - y_1(x, \omega)y_2'(x, \omega)). \quad (3)$$

For large ω the coefficients $a(\omega)$ and $b(\omega)$ satisfy the following asymptotic relations [6], valid for all ω with $\text{Im } \omega \geq 0$,

$$a(\omega) = 1 + \frac{I_q}{2i\omega} + o\left(\frac{1}{|\omega|}\right) \quad \text{and} \quad b(\omega) = o\left(\frac{1}{|\omega|}\right) \quad (4)$$

where $I_q := \int_{-\infty}^{\infty} q(x)dx$.

The transmission coefficient $a(\omega)$ may possess a finite number of simple purely imaginary zeros $\omega_1, \dots, \omega_m$ whose squares are the eigenvalues of the operator H . Denote by $v_1(x), \dots, v_m(x)$ the corresponding eigenfunctions of the discrete spectrum (their eigenvalues equal ω_j^2) with norm 1 in $L_2(\mathbb{R})$. Together with the set of solutions

$$\left\{ u_1(x, \omega) := \frac{y_1(x, \omega)}{\sqrt{2\pi a(\omega)}}, \quad u_2(x, \omega) := \frac{y_2(x, \omega)}{\sqrt{2\pi a(\omega)}} \right\} \quad (5)$$

they form a complete orthonormal system of generalized eigenfunctions of the operator H [4, Theorem 6.2]. The equality

$$\int_0^{\infty} \left(\overline{u_1(x, \omega)}u_1(y, \omega) + \overline{u_2(x, \omega)}u_2(y, \omega) \right) d\omega + \sum_{j=1}^m \overline{v_j(x)}v_j(y) = \delta(x - y)$$

understood in a distributional sense is valid.

The Green function of the operator $H - \lambda$ admits the representation (see, e.g., [7, Sect. 5.3])

$$G(x, y; \lambda) = \sum_{j=1}^m \frac{v_j(x)\overline{v_j(y)}}{\lambda_j - \lambda} + \int_0^{\infty} \frac{u_1(x, \omega)\overline{u_1(y, \omega)}}{\omega^2 - \lambda} d\omega + \int_0^{\infty} \frac{u_2(x, \omega)\overline{u_2(y, \omega)}}{\omega^2 - \lambda} d\omega, \quad (6)$$

$\lambda \notin [0, \infty) \cup \{\lambda_j\}_{j=1}^m$. In practice, the computation of the Green function is performed more frequently by means of the formula (see, e.g., [6])

$$G(x, y; \lambda) = \frac{y_1(x, \sqrt{\lambda})y_2(y, \sqrt{\lambda})}{2i\sqrt{\lambda}a(\sqrt{\lambda})}, \quad y < x, \quad (7)$$

$$G(x, y; \lambda) = G(y, x; \lambda) \quad (8)$$

where $\lambda \in \mathbb{C}$ and the branch for $\sqrt{\lambda}$ is chosen so that $\text{Im } \sqrt{\lambda} \geq 0$. If $\lambda \neq \omega_j^2$ and $\lambda \neq 0$ the following estimate holds

$$|G(x, y; \lambda)| \leq C e^{-\text{Im } \sqrt{\lambda}|x-y|}.$$

Often the Green function must be computed for λ being large negative numbers (see, e.g., [2], [3]). In this case formula (7) presents serious numerical difficulties due to the fact that one of the solutions is exponentially increasing while the other is exponentially decreasing, in both cases with $\sqrt{\lambda}$ participating in the exponential order. In spite of a seemingly more complicated appearance, formula (6) becomes more convenient for computation. However, usually the integrals appearing in it are not computed due to the obvious difficulty in calculating the solutions (5) for a large interval with respect to ω , and $G(x, y; \lambda)$ is approximated by the finite sum $\sum_{j=1}^m \frac{v_j(x)\overline{v_j(y)}}{\lambda_j - \lambda}$ only

(see, e.g., [2], [3]). Occasionally, in some practical models of wave propagation, such approximation can be justified with the aid of certain asymptotic considerations. Nevertheless, the interest in accurate computing of the Green function remains, and in the present work we show that formula (6) combined with the NSBF representation of solutions of (2) obtained in [12] offers a viable way to perform such computations.

3 NSBF representation for solutions of the one-dimensional Schrödinger equation

Throughout the paper we suppose that f is a non-vanishing solution (in general, complex-valued) of the equation

$$Hf = 0 \quad (9)$$

satisfying the initial condition

$$f(0) = 1.$$

Since q is real valued, such f can be chosen, e.g., as the following combination $f_0 + if_1$ of two solutions of (9) satisfying the initial conditions

$$f_0(0) = 1, \quad f_0'(0) = 0 \quad (10)$$

and

$$f_1(0) = 0, \quad f_1'(0) = 1.$$

Denote $h := f'(0)$.

Consider two sequences of recursive integrals (see [9], [11])

$$X^{(0)}(x) \equiv 1, \quad X^{(n)}(x) = n \int_0^x X^{(n-1)}(s) (f^2(s))^{(-1)^n} ds, \quad n = 1, 2, \dots$$

and

$$\tilde{X}^{(0)} \equiv 1, \quad \tilde{X}^{(n)}(x) = n \int_0^x \tilde{X}^{(n-1)}(s) (f^2(s))^{(-1)^{n-1}} ds, \quad n = 1, 2, \dots$$

Definition 1 *The families of functions $\{\varphi_k\}_{k=0}^\infty$ and $\{\psi_k\}_{k=0}^\infty$ constructed according to the rules*

$$\varphi_k(x) = \begin{cases} f(x)X^{(k)}(x), & k \text{ odd}, \\ f(x)\tilde{X}^{(k)}(x), & k \text{ even} \end{cases} \quad (11)$$

and

$$\psi_k(x) = \begin{cases} \frac{\tilde{X}^{(k)}(x)}{f(x)}, & k \text{ odd}, \\ \frac{X^{(k)}(x)}{f(x)}, & k \text{ even}. \end{cases} \quad (12)$$

are called the systems of formal powers associated with f .

Remark 2 *The formal powers arise in the spectral parameter power series (SPPS) representation for solutions of (2) (see [8], [9], [10], [11]).*

Let $c(x, \omega)$, $s(x, \omega)$ denote the solutions of (2) satisfying the initial conditions in the origin

$$c(0, \omega) = 1, \quad c'(0, \omega) = h, \quad s(0, \omega) = 0, \quad s'(0, \omega) = \omega, \quad (13)$$

where $h = f'(0) \in \mathbb{C}$.

Theorem 3 ([12]) *The solutions $c(x, \omega)$ and $s(x, \omega)$ of (2) admit the following representations*

$$c(x, \omega) = \cos \omega x + 2 \sum_{n=0}^{\infty} (-1)^n \beta_{2n}(x) j_{2n}(\omega x) \quad (14)$$

and

$$s(x, \omega) = \sin \omega x + 2 \sum_{n=0}^{\infty} (-1)^n \beta_{2n+1}(x) j_{2n+1}(\omega x), \quad (15)$$

where j_m stands for the spherical Bessel function of order m , the functions β_n are defined as follows

$$\beta_n(x) = \frac{2n+1}{2} \left(\sum_{k=0}^n \frac{l_{k,n} \varphi_k(x)}{x^k} - 1 \right), \quad (16)$$

where $l_{k,n}$ is the coefficient of x^k in the Legendre polynomial of order n . The series in (14) and (15) converge uniformly with respect to x on any segment and converge uniformly with respect to ω on any compact subset of the complex plane of the variable ω . Moreover, for the functions

$$c_N(x, \omega) = \cos \omega x + 2 \sum_{n=0}^N (-1)^n \beta_{2n}(x) j_{2n}(\omega x) \quad (17)$$

and

$$s_N(x, \omega) = \sin \omega x + 2 \sum_{n=0}^N (-1)^n \beta_{2n+1}(x) j_{2n+1}(\omega x) \quad (18)$$

the following estimates hold

$$|c(x, \omega) - c_N(x, \omega)| \leq 2|x|\varepsilon_N(x) \quad \text{and} \quad |s(x, \omega) - s_N(x, \omega)| \leq 2|x|\varepsilon_N(x) \quad (19)$$

for any $\omega \in \mathbb{R}$, $\omega \neq 0$, and

$$|c(x, \omega) - c_N(x, \omega)| \leq \frac{2\varepsilon_N(x) \sinh(Cx)}{C} \quad \text{and} \quad |s(x, \omega) - s_N(x, \omega)| \leq \frac{2\varepsilon_N(x) \sinh(Cx)}{C} \quad (20)$$

for any $\omega \in \mathbb{C}$, $\omega \neq 0$ belonging to the strip $|\operatorname{Im} \omega| \leq C$, $C \geq 0$, where ε_N is a nonnegative function decreasing to zero as $N \rightarrow \infty$ (an estimate for $\varepsilon_N(x)$ is presented in [12]).

Theorem 4 ([12]) *The derivatives of the solutions $c(x, \omega)$ and $s(x, \omega)$ with respect to x admit the following representations*

$$c'(x, \omega) = -\omega \sin \omega x + \left(h + \frac{1}{2} \int_0^x q(s) ds \right) \cos \omega x + 2 \sum_{n=0}^{\infty} (-1)^n \gamma_{2n}(x) j_{2n}(\omega x) \quad (21)$$

and

$$s'(x, \omega) = \omega \cos \omega x + \frac{1}{2} \left(\int_0^x q(s) ds \right) \sin \omega x + 2 \sum_{n=0}^{\infty} (-1)^n \gamma_{2n+1}(x) j_{2n+1}(\omega x) \quad (22)$$

where γ_n are defined as follows

$$\gamma_n(x) = \frac{2n+1}{2} \left(\sum_{k=0}^n \frac{l_{k,n}}{x^k} \left(k \psi_{k-1}(x) + \frac{f'(x) \varphi_k(x)}{f(x)} \right) - \frac{n(n+1)}{2x} - \frac{1}{2} \int_0^x q(s) ds - \frac{h}{2} (1 + (-1)^n) \right). \quad (23)$$

The series in (21) and (22) converge uniformly with respect to x on any segment and converge uniformly with respect to ω on any compact subset of the complex plane of the variable ω .

Moreover, for the approximations

$$\mathring{c}_N(x, \omega) := -\omega \sin \omega x + \left(h + \frac{1}{2} \int_0^x q(s) ds \right) \cos \omega x + 2 \sum_{n=0}^N (-1)^n \gamma_{2n}(x) j_{2n}(\omega x) \quad (24)$$

and

$$\mathring{s}_N(x, \omega) := \omega \cos \omega x + \frac{1}{2} \left(\int_0^x q(s) ds \right) \sin \omega x + 2 \sum_{n=0}^N (-1)^n \gamma_{2n+1}(x) j_{2n+1}(\omega x) \quad (25)$$

the following inequalities are valid

$$\left| c'(x, \omega) - \mathring{c}_N(x, \omega) \right| \leq 2|x|\varepsilon_{1,N}(x) \quad \text{and} \quad \left| s'(x, \omega) - \mathring{s}_N(x, \omega) \right| \leq 2|x|\varepsilon_{1,N}(x)$$

for any $\omega \in \mathbb{R}$, $\omega \neq 0$, and

$$\left| c'(x, \omega) - \mathring{c}_N(x, \omega) \right| \leq \frac{2\varepsilon_{1,N}(x) \sinh(Cx)}{C} \quad \text{and} \quad \left| s'(x, \omega) - \mathring{s}_N(x, \omega) \right| \leq \frac{2\varepsilon_{1,N}(x) \sinh(Cx)}{C}$$

for any $\omega \in \mathbb{C}$, $\omega \neq 0$ belonging to the strip $|\operatorname{Im} \omega| \leq C$, $C \geq 0$, where $\varepsilon_{1,N}$ is a nonnegative function decreasing to zero as $N \rightarrow \infty$.

Remark 5 The inequalities (19) and (20) are of particular importance when using representations (14) and (15) because they guarantee a uniform (ω -independent) error estimate for an approximation of solutions which was illustrated by numerical experiments in [12].

Remark 6 For numerical implementation of the NSBF representations the formulas (16) and (23) are not the best options. Due to the fast growth of the Legendre polynomial's coefficients only few functions β_n and γ_n can be computed with sufficient accuracy. Better option consists in using the alternative recurrent formulas proposed in [12, Section 6].

4 Construction of the Jost solutions

The condition (1) indicates a sufficiently fast decay of $|q(x)|$ when $|x| \rightarrow \infty$. This means that a compactly supported potential can be a reasonable approximation of q . Let us consider the operator H with a compactly supported potential q , and without loss of generality suppose that $\operatorname{supp} q \subset [0, d]$, $d > 0$. Then the solution $y_2(x, \omega)$ satisfies the initial conditions

$$y_2(0, \omega) = 1 \quad \text{and} \quad y_2'(0, \omega) = -i\omega, \quad (26)$$

while the initial conditions for $y_1(x, \omega)$ at the point d have the form

$$y_1(d, \omega) = e^{i\omega d} \quad \text{and} \quad y_1'(d, \omega) = i\omega e^{i\omega d}. \quad (27)$$

We are looking for $y_1(x, \omega)$ and $y_2(x, \omega)$ in the form of linear combinations of $c(x, \omega)$ and $s(x, \omega)$. Since

$$c(0, \omega) = 1, \quad c'(0, \omega) = h, \quad s(0, \omega) = 0, \quad s'(0, \omega) = \omega$$

we obtain

$$y_1(x, \omega) = \frac{e^{i\omega d}}{\omega} \left((s'(d, \omega) - i\omega s(d, \omega)) c(x, \omega) + (i\omega c(d, \omega) - c'(d, \omega)) s(x, \omega) \right) \quad (28)$$

and

$$y_2(x, \omega) = c(x, \omega) - is(x, \omega) - \frac{h}{\omega} s(x, \omega). \quad (29)$$

Thus, we are in a position to use the NSBF representation for computing $a(\omega)$ and the orthonormalized eigenfunctions of the continuous spectrum (5) as well as the orthonormalized eigenfunctions of the discrete spectrum $v_1(x), \dots, v_m(x)$ (which can also be calculated using the SPSS method described in [5]). Taking into account that $a(\omega)$ can be singular in the origin it is convenient to calculate the values of the functions (5) for $\omega = 0$. This result we formulate in the following statement.

Theorem 7 *Let q be real valued, $\text{supp } q \subset [0, d]$, $d > 0$ and $q \in C[0, d]$. Then the following asymptotic relation is valid*

$$a(\omega) = \frac{f_0'(d)}{2i\omega} - \frac{1}{2} (f_0(d) - df_0'(d) + \varphi_1'(d)) + O(\omega) \quad \text{when } \omega \rightarrow 0 \quad (30)$$

where f_0 satisfies (9) and (10).

The transmission coefficient $a(\omega)$ has a simple pole in the origin if and only if zero is not a Neumann eigenvalue of the operator H on $[0, d]$, and in this case

$$u_1(x, 0) = u_2(x, 0) = 0. \quad (31)$$

Otherwise,

$$a(\omega) = -\frac{1}{2} (f_0(d) + \varphi_1'(d)) + O(\omega) \quad \text{when } \omega \rightarrow 0, \quad (32)$$

$f_0(d) + \varphi_1'(d) \neq 0$, and

$$u_1(x, 0) = -\sqrt{\frac{2}{\pi}} \frac{f_0(x)}{f_0^2(d) + 1} \quad \text{and} \quad u_2(x, 0) = -\sqrt{\frac{2}{\pi}} \frac{f_0(x)f_0(d)}{f_0^2(d) + 1}. \quad (33)$$

Proof. From the NSBF representations (14), (15) and (21), (22) of the solutions $c(x, \omega)$ and $s(x, \omega)$ and their derivatives as well as from formulas from [12] we find that

$$\begin{aligned} c(x, \omega) &= f(x) + O(\omega^2), & s(x, \omega) &= \varphi_1(x)\omega + O(\omega^3), \\ c'(x, \omega) &= f'(x) + O(\omega^2), & s'(x, \omega) &= \varphi_1'(x)\omega + O(\omega^3), \end{aligned} \quad \text{when } \omega \rightarrow 0$$

and hence

$$\begin{aligned} y_1(x, \omega) &= f(x)\varphi_1'(d) - f'(d)\varphi_1(x) \\ &\quad + i\omega \left(f(d)\varphi_1(x) - f(x)\varphi_1(d) + d(f(x)\varphi_1'(d) - f'(d)\varphi_1(x)) \right) + O(\omega^2), \\ y_2(x, \omega) &= f(x) - h\varphi_1(x) - i\varphi_1(x)\omega + O(\omega^2), \quad \text{when } \omega \rightarrow 0. \end{aligned}$$

Thus, from (3) we obtain

$$a(\omega) = \frac{f'(d) - h\varphi_1'(d)}{2i\omega} - \frac{1}{2} \left(f(d) - h\varphi_1(d) - d(f'(d) - h\varphi_1'(d)) + \varphi_1'(d) \right) + O(\omega) \quad \text{when } \omega \rightarrow 0. \quad (34)$$

Notice that the magnitude $f(d) - h\varphi_1(d)$ is invariant with respect to the choice of the particular solution $f(x)$ satisfying the condition $f(0) = 1$, see [13, Proposition 4.7]. In particular, for f_0 (34) takes the form (30), from which we see that $a(\omega)$ has a simple pole in the origin iff $f_0'(d) \neq 0$, that is, iff zero is not a Neumann eigenvalue of the operator H on $[0, d]$. In this case we obtain (31).

Consider the opposite situation when $f'_0(d) = 0$. It is easy to see that in this case $f_0(d) + \varphi'_1(d) \neq 0$. Indeed, when $f'_0(d) = 0$, we have that $\varphi'_1(d) = 1/f_0(d)$ ($f_0(d) \neq 0$ due to the uniqueness of the solution of the Cauchy problem). The expression $f_0(d) + 1/f_0(d) \neq 0$ because otherwise $f_0(d) = \pm i$ which is impossible due to the real-valuedness of q . Thus, iff zero is a Neumann eigenvalue of the operator H on $[0, d]$ the asymptotic behaviour of the transmission coefficient $a(\omega)$ when $\omega \rightarrow 0$ is described by (32) where the first term of the asymptotics is different from zero. Consequently, in this case the relations (33) hold. ■

Example 8 Consider the potential

$$q(x) = \begin{cases} C, & x \in [0, d] \\ 0, & x \notin [0, d] \end{cases}$$

where C is a real constant. Take $h = 0$. A simple calculation leads to the following relations

$$c(x, \omega) = \cos \alpha x, \quad s(x, \omega) = \frac{\omega}{\alpha} \sin \alpha x,$$

where $\alpha := \sqrt{\omega^2 - C}$, and

$$\begin{aligned} y_1(x, \omega) &= e^{i\omega d} \left(\cos \alpha (d - x) - \frac{i\omega}{\alpha} \sin \alpha (d - x) \right), \\ y'_1(x, \omega) &= e^{i\omega d} (\alpha \sin \alpha (d - x) + i\omega \cos \alpha (d - x)), \\ y_2(x, \omega) &= \cos \alpha x - \frac{i\omega}{\alpha} \sin \alpha x, \\ y'_2(x, \omega) &= -\alpha \sin \alpha x - i\omega \cos \alpha x. \end{aligned}$$

Calculation of $a(\omega)$ according to (3) gives us the following expression

$$a(\omega) = -e^{i\omega d} \left(\cos \alpha d + \frac{\omega^2 + \alpha^2}{2i\omega\alpha} \sin \alpha d \right). \quad (35)$$

From here as well as by means of (30) it can be seen that $a(\omega)$ has a simple pole in the origin except when $\sin(i\sqrt{C}d) = 0$. This is possible if only $C < 0$ and d is such that $\sqrt{-C}d = n\pi$, $n \in \mathbb{Z}$.

Note that with the aid of (7) and (8) the Green function can be written in the form

$$\begin{aligned} G(x, y; \omega^2) &= \frac{e^{i\omega d}}{2i\omega a(\omega)} \left(\cos \alpha (d - x + y) - \frac{i\omega}{\alpha} \sin \alpha (d - x + y) \right. \\ &\quad \left. - \frac{C}{\alpha^2} \sin \alpha (d - x) \sin \alpha y \right), \quad y < x, \end{aligned}$$

which together with (8) defines it for all values of x and y . Here $a(\omega)$ is defined by (35).

5 Improving the convergence of the integrals in (6)

The solutions $c(x, \omega)$ and $s(x, \omega)$ satisfying the initial conditions (13) possess the following asymptotics for real values of ω (see, e.g., [15, Section 1.1], see also formulas (5.2) and (5.3) from [12])

$$c(x, \omega) = \cos \omega x + \left(h + \frac{Q(x)}{2} \right) \frac{\sin \omega x}{\omega} + o(1/\omega), \quad (36)$$

$$c'(x, \omega) = -\omega \sin \omega x + \left(h + \frac{Q(x)}{2} \right) \cos \omega x + o(1), \quad (37)$$

$$s(x, \omega) = \sin \omega x - \frac{Q(x)}{2} \frac{\cos \omega x}{\omega} + o(1/\omega), \quad (38)$$

$$s'(x, \omega) = \omega \cos \omega x + \frac{Q(x)}{2} \sin \omega x + o(1), \quad \omega \rightarrow \pm\infty, \quad (39)$$

where

$$Q(x) := \int_0^x q(t) dt.$$

For absolutely continuous on $[0, d]$ potentials the error terms $o(1/\omega)$ and $o(1)$ can be changed to $O(1/\omega^2)$ and $O(1/\omega)$, respectively. Using this asymptotics as well as (4) and formulas (28) and (29) one can verify that the integrands from (6) possess the following asymptotics

$$\begin{aligned} u_1(x, \omega) \overline{u_1(y, \omega)} + u_2(x, \omega) \overline{u_2(y, \omega)} &= \frac{y_1(x, \omega) \overline{y_1(y, \omega)} + y_2(x, \omega) \overline{y_2(y, \omega)}}{2\pi |a(\omega)|^2} \\ &= \frac{2 \cos \omega(x-y) + \frac{(Q(x)-Q(y)) \sin \omega(x-y)}{\omega} + o(1/\omega)}{2\pi |a(\omega)|^2} \\ &= \frac{\cos \omega(x-y)}{\pi} + \frac{(Q(x) - Q(y)) \sin \omega(x-y)}{2\pi\omega} + o\left(\frac{1}{\omega}\right), \\ &\quad \omega \rightarrow +\infty. \end{aligned} \quad (40)$$

Again, for absolutely continuous on $[0, d]$ potentials the error term can be changed to $O(1/\omega^2)$.

The asymptotic relation (40) explains the slow convergence of the integrals in (6), the integrands decay as $1/\omega^2$ as $\omega \rightarrow +\infty$. At the same time, it provides the way to improve the convergence rate. Note that (c.f., formulas 2.5.9.5, 2.5.9.10 and 2.5.9.11 from [14])

$$\int_0^\infty \frac{\cos \omega(x-y)}{\pi(\omega^2 - \lambda)} d\omega = -\frac{e^{i|x-y|\sqrt{\lambda}}}{2i\sqrt{\lambda}},$$

where the branch for $\sqrt{\lambda}$ is chosen so that $\text{Im} \sqrt{\lambda} > 0$ (such branch is uniquely defined since the formula (6) can be used only for $\lambda \notin [0, \infty)$), and

$$\begin{aligned} \int_0^\infty \frac{\sin \omega|x-y|}{2\pi\omega(\omega^2 - \lambda)} d\omega &= \int_0^\infty \frac{(\omega^2 - \lambda) \sin \omega|x-y|}{2\pi\omega(\omega^2 - \lambda)^2} d\omega \\ &= \int_0^\infty \frac{\omega \sin \omega|x-y|}{2\pi(\omega^2 - \lambda)^2} d\omega - \int_0^\infty \frac{\lambda \sin \omega|x-y|}{2\pi\omega(\omega^2 - \lambda)^2} d\omega \\ &= -\frac{|x-y|e^{i|x-y|\sqrt{\lambda}}}{8i\sqrt{\lambda}} - \frac{1}{4\lambda} + \frac{e^{i|x-y|\sqrt{\lambda}}}{4\lambda} + \frac{|x-y|e^{i|x-y|\sqrt{\lambda}}}{8i\sqrt{\lambda}} \\ &= \frac{e^{i|x-y|\sqrt{\lambda}} - 1}{4\lambda}. \end{aligned}$$

Hence we may rewrite the formula (6) either as

$$\begin{aligned} G(x, y; \lambda) &= \sum_{j=1}^m \frac{v_j(x) \overline{v_j(y)}}{\lambda_j - \lambda} - \frac{e^{i|x-y|\sqrt{\lambda}}}{2i\sqrt{\lambda}} \\ &\quad + \int_0^\infty \frac{u_1(x, \omega) \overline{u_1(y, \omega)} + u_2(x, \omega) \overline{u_2(y, \omega)} - \frac{1}{\pi} \cos \omega(x-y)}{\omega^2 - \lambda} d\omega \end{aligned} \quad (41)$$

or as

$$\begin{aligned} G(x, y; \lambda) &= \sum_{j=1}^m \frac{v_j(x) \overline{v_j(y)}}{\lambda_j - \lambda} - \frac{e^{i|x-y|\sqrt{\lambda}}}{2i\sqrt{\lambda}} + \frac{e^{i|x-y|\sqrt{\lambda}} - 1}{4\lambda} \cdot \frac{x-y}{|x-y|} (Q(x) - Q(y)) \\ &\quad + \int_0^\infty \frac{u_1(x, \omega) \overline{u_1(y, \omega)} + u_2(x, \omega) \overline{u_2(y, \omega)} - \frac{2\omega \cos \omega(x-y) + (Q(x) - Q(y)) \sin \omega(x-y)}{2\pi\omega}}{\omega^2 - \lambda} d\omega. \end{aligned} \quad (42)$$

Now the integrand in (41) can be estimated by the expression $1/\omega^3$ as $\omega \rightarrow +\infty$, while in (42) (for absolutely continuous on $[0, d]$ potentials) by the expression $1/\omega^4$ resulting in a faster integral's convergence. We give a numerical illustration in Section 6.

6 Numerical implementation

The procedure for the computation of the Green function based on the NSBF representations was implemented using Matlab 2017a. The first step is to compute a nonvanishing solution f of (9) together with its first derivative (see [9], [11] for details). Then the systems of formal powers (11) and (12) associated to f are computed. Next, a number of the functions β_k , and γ_k are computed according to Remark 6 which lead to the approximate NSBF representations $c_N(x, \omega)$ and $s_N(x, \omega)$ of solutions (see (17) and (18)) as well as of their derivatives (24) and (25). Then the Jost solutions $y_1(x, \omega)$ and $y_2(x, \omega)$ can be computed using (28) and (29), which allow one to compute $u_1(x, \omega)$ and $u_2(x, \omega)$ and hence $G(x, y; \lambda)$ with the aid of (42). Since the main difficulty usually consists in computing the integrals in (42), we consider an example void of a discrete spectrum.

Notice that to compute the Green function for any value of $\lambda =: \omega_c^2$ not belonging to the spectrum of H the integration in formula (42) requires the solutions $u_1(x, \omega)$ and $u_2(x, \omega)$ to be computed for $\omega \in [0, \infty)$ only. Here is where the independence with respect to $\omega \in \mathbb{R}$ of the estimate of the approximation (see (19)) becomes especially attractive.

Computations were performed for the case considered in Example 8 with $C = 1$ and $d = 1$. On the segment $x \in [0, d]$ equally spaced 1001 points have been chosen for the representation of all the functions involved, 30 formal powers have been computed for the construction of f , and N was set as 12 (for details see [12, Remark 7.1]).

First, we illustrate the slow convergence of the integrals in (6) and compare the improvements achieved by using (41) and (42). The numerical integration was performed by truncating the integrals for $\omega = \Omega$, $\Omega \leq 10^5$ and using the six points Newton-Cotes method of seventh order and the step of 0.01. The Green function was computed for two cases, $x = 0.97$, $y = 0.069$ (distant points x and y) and $x = 0.97$, $y = 0.969$ (close points x and y) and $\lambda = -4$.

The convergence of the integrals in (6) is slow as can be seen on Fig. 1. For distant points x and y the second improvement formula (42) is considerably better giving 2 orders of ω faster decay of the integral truncation error. However for close values of x and y one can use the first improvement formula (41) as well, thanks to the smallness of the contribution of the second asymptotic term in (40). In both cases the error stabilizes on the values of the truncation parameter Ω of about 10^4 , which we will use for all further computations.

The absolute error dependence on x for the NSBF method is shown on Figure 2 achieving its maximum in the neighborhood of the point $x = y$.

Finally, the maximum absolute error for the Green function computed on a domain of the complex plane of the variable ω_c is shown on Figure 3. As can be seen the absolute error of the approximation obtained with the aid of the method proposed here and based on (42) and NSBF representations is uniform with the exception of a small neighborhood of $\omega_c = 0$.

For comparison the Green function was also computed by formulas (7) and (8) with the aid of Matlab's `ode45` solver. Note that the computation of the solution y_1 by the Matlab solver requires some care. First, since the solution y_1 is decreasing, it should be computed "from right to left" starting from the initial conditions (27). Second, the initial value $e^{i\omega d}$ is very small for the values of ω having large positive imaginary part. In order to obtain a good accuracy from the `ode45` solver, one either has to specify a very small (say, $10^{-15} \cdot e^{-\text{Im}\omega d}$) value for the 'AbsTol' parameter or to rescale the initial value, setting $\tilde{y}(d) = 1$, $\tilde{y}'(d) = i\omega$ and then multiplying the returned function by

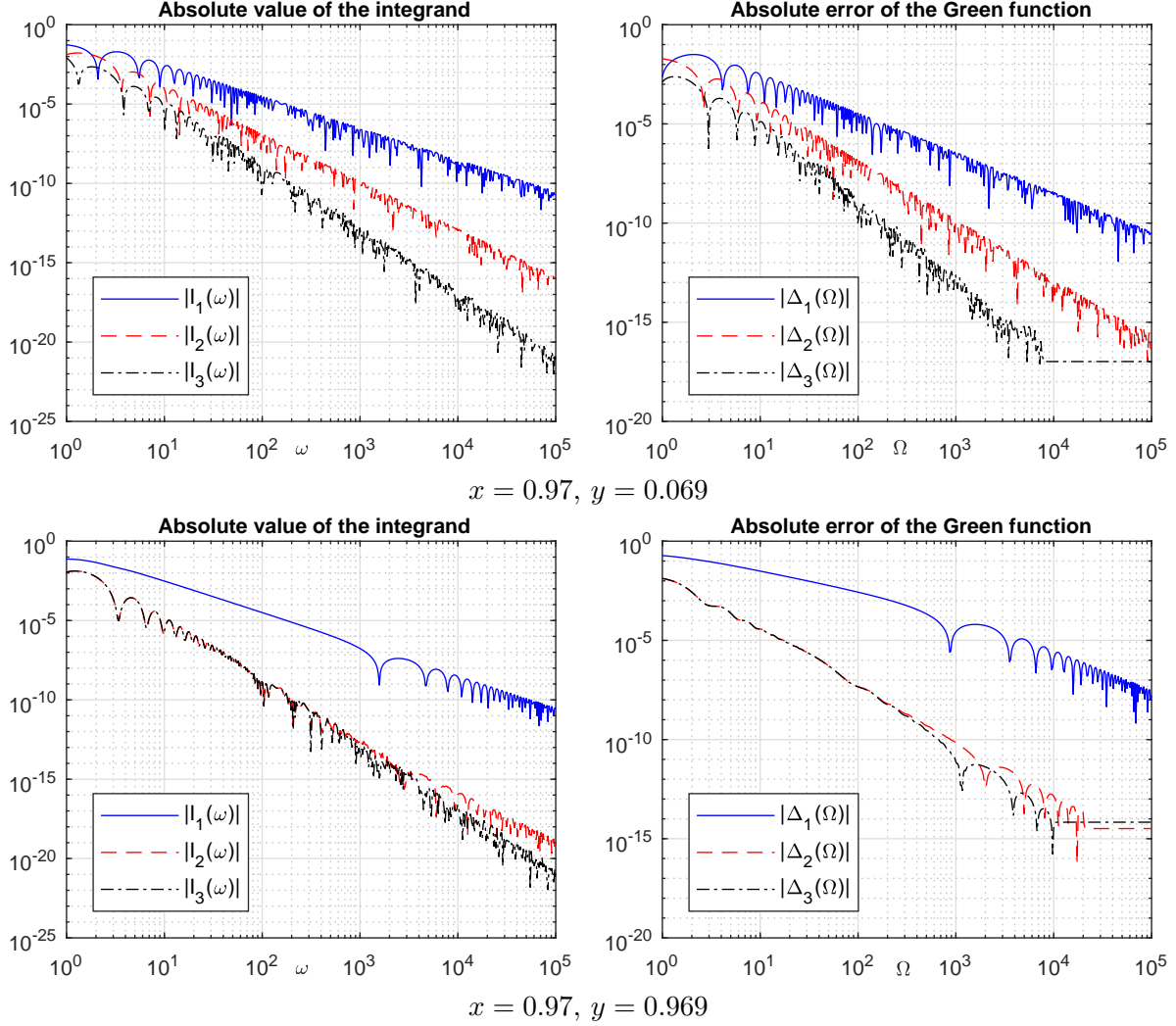


Figure 1: Top left: absolute values of the integrands (I_1 – the sum of the integrands from (6), I_2 – the integrand from (41) and I_3 – the integrand from (42)) for distant points $x = 0.97, y = 0.069$. Bottom left: absolute values of the same integrands for close points $x = 0.97, y = 0.969$. Top right: absolute errors of the computed Green function for distant points $x = 0.97, y = 0.069$ (Δ_1 – using formula (6), Δ_2 – using formula (41) and Δ_3 – using formula (42)) as the functions of the upper limit Ω chosen to truncate the integrals. Bottom right: same absolute errors of the computed Green function for close points $x = 0.97, y = 0.969$.

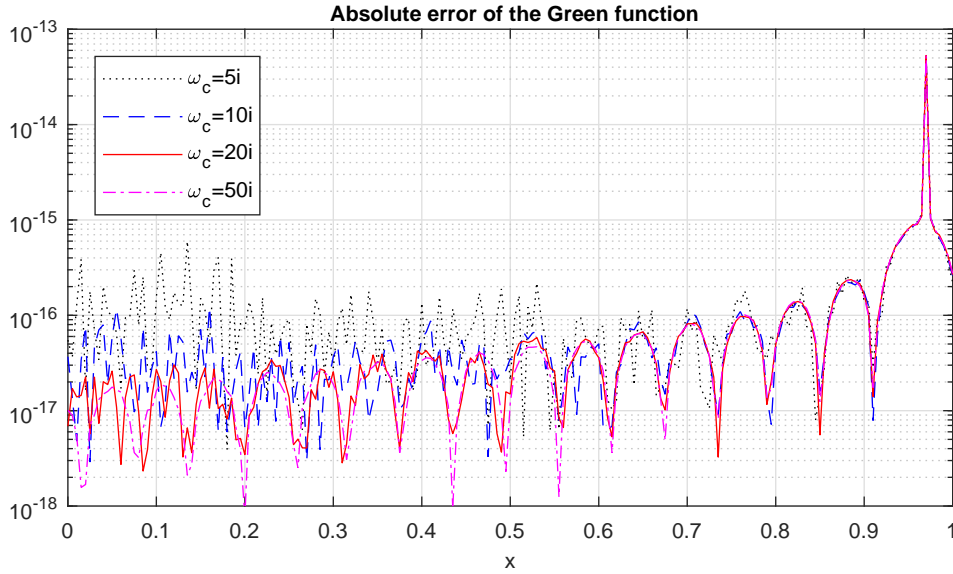


Figure 2: Absolute error of the Green function $G(x, 0.97; \omega_c^2)$ computed using (42) for different values of ω_c .

$e^{i\omega d}$. Once the computation was performed correctly, the maximum absolute errors of the computed Green function by the proposed method and by the `ode45` solver were comparable.

Conclusions

A method for computation of the Green function for the one-dimensional Schrödinger equation is proposed based on the eigenfunction expansion of the Green function and the NSBF representations of the generalized eigenfunctions. It proved to be a stable and accurate method comparable with the representation in terms of two Jost solutions computed by the `ode45` solver provided by Matlab.

Acknowledgements

R. Castillo would like to thank the support of Instituto Politécnico Nacional through a sabbatical year. Research of V. Kravchenko and S. Torba was partially supported by CONACYT, Mexico via the projects 284470 and 222478.

References

- [1] M. J. Ablowitz, P. A. Clarkson, *Solitons, Nonlinear Evolution Equations and Inverse Scattering*, London Math. Soc. Lecture Note Series, 149. Cambridge University Press, 1991.
- [2] V. Barrera-Figueroa, V. V. Kravchenko, V. S. Rabinovich, *Spectral parameter power series analysis of isotropic planarly layered waveguides*, *Appl. Anal.* 93 (2014), no. 4, 729–755.
- [3] V. Barrera-Figueroa, V. S. Rabinovich, *Asymptotics of the far field generated by a modulated point source in a planarly layered electromagnetic waveguide*, *Math. Methods Appl. Sci.* 38 (2015), no. 10, 1970–1989.
- [4] F. A. Berezin, M. A. Shubin, *The Schrödinger equation*, Kluwer Academic Publishers Group, Dordrecht, 1991.

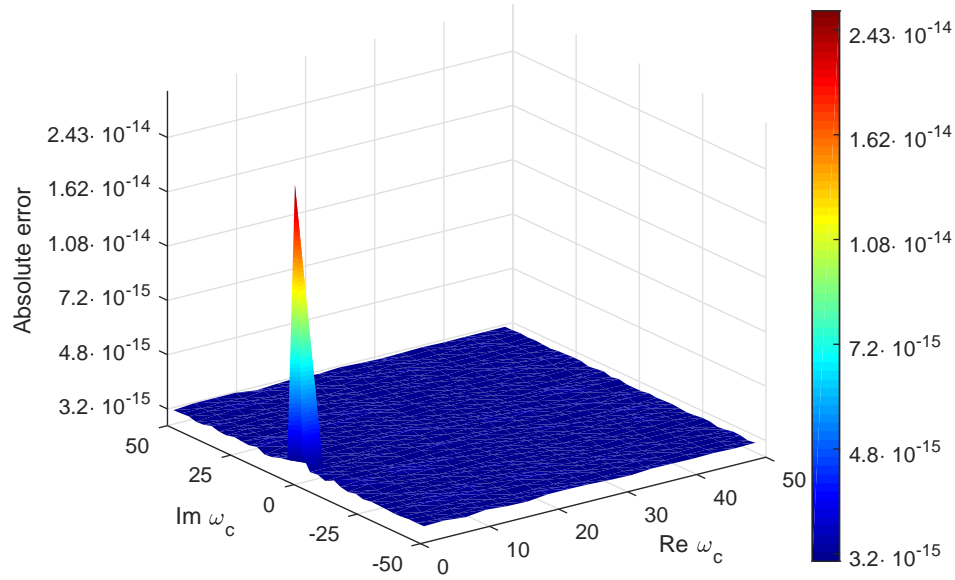


Figure 3: The maximum with respect to x absolute error of the Green function $G(x, 0.97; \omega_c^2)$ computed using (42) on a domain of the complex plane of the variable ω_c .

- [5] R. Castillo-Perez, V. V. Kravchenko, H. Oviedo, V. S. Rabinovich, *Dispersion equation and eigenvalues for quantum wells using spectral parameter power series*, J. Math. Phys. 52, 043522, 2011.
- [6] L. D. Faddeev, *The inverse problem in the quantum theory of scattering. II*, J. Soviet Math. 5:3 (1976), 334–396.
- [7] G. W. Hanson, A. B. Yakovlev, *Operator Theory for Electromagnetics: An Introduction*, Springer; 2002.
- [8] K. V. Khmelnyskaya, V. V. Kravchenko and H. C. Rosu, *Eigenvalue problems, spectral parameter power series, and modern applications*, Math. Methods Appl. Sci. 38 (2015), 1945–1969.
- [9] V. V. Kravchenko, *A representation for solutions of the Sturm-Liouville equation*, Complex Var. Elliptic Equ. 53 (2008), 775–789.
- [10] V. V. Kravchenko, S. Morelos and S. Tremblay, *Complete systems of recursive integrals and Taylor series for solutions of Sturm-Liouville equations*, Math. Methods Appl. Sci. 35 (2012), 704–715.
- [11] V. V. Kravchenko and R. M. Porter, *Spectral parameter power series for Sturm-Liouville problems*, Math. Methods Appl. Sci. 33 (2010), 459–468.
- [12] V. V. Kravchenko, L. J. Navarro and S. M. Torba, *Representation of solutions to the one-dimensional Schrödinger equation in terms of Neumann series of Bessel functions*, Appl. Math. Comp. 314 (2017), 173–192.
- [13] V. V. Kravchenko and S. M. Torba, *Transmutations and spectral parameter power series in eigenvalue problems*, Operator Theory: Advances and Applications, 228 (2013), 209–238.
- [14] A. P. Prudnikov, Yu. A. Brychkov and O. I. Marichev, *Integrals and series. Vol. 2. Special functions*, New York: Gordon & Breach Science Publishers, 1986.
- [15] V. A. Yurko, *Method of Spectral Mappings in the Inverse Problem Theory*, Berlin, Boston: De Gruyter, 2002.